A Design Configuration and Optimization for a Multi Rotor UAV

Elisa Capello, Giorgio Guglieri, Fulvia Quagliotti

Politecnico di Torino – DIASP
Corso Duca degli Abruzzi 24
10129 Torino (Italy)
elisa.capello@polito.it -fulvia.quagliotti@polito.it - giorgio.guglieri@polito.it

ABSTRACT

Multi rotor UAVs offer great potential wide range of challenging applications due to the high manoeuvrability and to the potential to hover, take off and fly in small areas. Nevertheless, their design is in some way critical. The main concern is their inadequate level of handling qualities due to the intrinsic instabilities of this type of small size vehicles. A specific hardware with a control matrix is also required to stabilize and manoeuvre the aircraft. A non-marginal trust-to-weight ratio is mandatory that implies adequate sizing of the power output provided by the propulsion system, generally compromising their endurance and their payload capabilities. In the last years, in the attempt to overcome these issues, several multi rotor unmanned vehicles have been developed. The aim of the present project is to create a compact, robust and highly manoeuvrable autonomous UAV. The quad-rotor ELISA (intEgrated muLtI-rotor for Surveillance Applications) is controlled by changing the rotation speed of the motors. The torque in the yaw direction is cancelled by spinning two of the propellers clockwise and the other two anti-clockwise.

The optimal configuration has been chosen in order to increase the aircraft structural stiffness and to enhance the stability and the controllability of the vehicle. The mini-rotors are supported by a set of equally spaced composite radial bars, each of them linked with a central payload case.

The research steps presented in this paper concern the analysis of the vehicle configuration and the definition of the mathematical model describing the dynamic behaviour..

Main results of this work will be reported and widely discussed in the paper.

1.0 INTRODUCTION

Rotary-wing UAVs can have capabilities to perform missions that can not be achieved with fixed-wing UAVs. Rotary-wing vehicles have the potential to be very useful in territorial monitoring and, especially in the last years, R/C helicopters are used for aerial survey.

Many University research groups have developed rotary-wing systems, even if today the widespread research and use is almost reserved to military organizations. Recently, the University of Maryland has also developed two rotary- wing micro UAVs [1]. This micro vehicle has two counter-rotating coaxial rotors and weights 140 grams.

Small rotary-wing UAVs with VTOL and hover capabilities can have many applications; these UAVs could be especially useful for indoor flight or for urban missions. Using UAVs for reconnaissance in these situations is also challenging because of the short line of sight and many obstacles. They are able to fly in areas with obstacles and poor quality GPS signals.
Incorporating a reliable semi-autonomous or autonomous control system in these small vehicles, the operator does not have to constantly monitor the platform flight parameters or location. However the on board software will have to be very compact to fit in the available memory of the small microprocessors,

but powerful enough to provide control with sensor data of limited quality.

These vehicles can be very challenging. Recently, a quad-rotor is a rotary wing UAV that has been the subject of several recent research projects. Small quad-rotors have many exciting potential missions including flight indoors and in urban areas. However, the development of the control systems needed to fly.

The most known quad-rotor is the Draganflyer [2], a commercial product from RC Toys; this vehicle is flown using an R/C transmitter and its onboard electronics. The pilot can control the throttle setting for the four motors and the yaw, pitch and roll rates of the platform. The recent version of Draganflyer includes four infrared heat sensors to allow the quad-rotor to level itself while it is being flown outdoors.

Another platform is the EADS Quattrocopter, used as a testbed for developing micro air vehicle flight control [3]. The Quattrocopter is capable of 20 minute flight with a single charge of its lithium batteries. The vehicle is length 65 cm, weights about half a kilogram and its detectable fuselage can be stored in a backpack. The electric motors allow this UAV to operate quietly.

Under development in Australia the X-4 flyer [4] has a frame length of 70 cm and weights 2 kg with almost 20 cm diameter rotors. The first flight testing was conducted using a truck battery and tether chord to provide power to the platform. However, these tests were not successful and the trust margin of the X-4 flyer was not large enough to allow controllable flight. The next goals for improvement are to design a new X-4 flyer that would be capable to produce more thrust with a wireless serial link and a camera system.

Research teams in some Universities are developing quad-rotor system control, starting from commercial available model. For example, a research team from France employed the commercial Draganflyer to study its stabilization [5]. In the same direction, a research group at the University of Pennsylvania is developing a quad-rotor using the commercial model HMX-4. Due to the weight limitations, no GPS or additional accelerometers could be placed on the platform.

At the Cornel University two quad-rotor projects have been performed. The goal of the first project was to develop a method to estimate the attitude of a vehicle by using an offboard vision system and three onboard gyroscopes [6]. The second project was concentrated on the four thrust producing units and structure of a quad-rotor. These two areas were especially important since this quad-rotor was heavier (6.2 kg) than the previously mentioned designs.

At the Aerospace Engineering Department (DIASP) of Politecnico di Torino, the Flight Mechanics Group is working on the development of a quad-rotor for the territorial monitoring and the map project for a dead zone and/or a grey area. The research is oriented to analyze how work and how maneuver this kind of platform. In order to better understand this problem, considering the dynamic equations and the performance, trying to improve the configuration, we have to realize the aircraft.
The research principle scope is to optimize the automatic control of a multi quad-rotors in formation flight, providing these platforms with a mini autopilot.

2.0 MODEL DESCRIPTION

This paper is focused on the design and the mathematical model of a four-rotor flying vehicle. A quadrotor is mechanically simple and is controlled only changing the speed of rotation of the four driving motors. The torque in the yaw direction is cancelled by spinning two of the rotors clockwise and the other two anti-clockwise. The attitude control in roll, pitch and yaw direction is obtained by varying the rotational speed, which eliminates the mechanical complexity of a pitch linkage. So the four rotor units do not require cyclic and collective pitch commands. The total thrust is controlled with the simultaneous variation of all rotor speed.

The optimal configuration has been chosen according to minimize the aircraft weight and to optimize the control strategy of the platform, taking into account the aircraft structural stiffness. A symmetric cruciform layout with peripheral propulsion units was selected in order to simplify the balance of the separate thrusters.

We can pick out between two options; one configuration has the four rotors connected to the central fuselage by four separate composite bars. In the second case, the mini-rotors can be supported by a set of equally spaced composite radial bars, reinforced by a square frame, each of them linked with the central payload case (Fig.1).

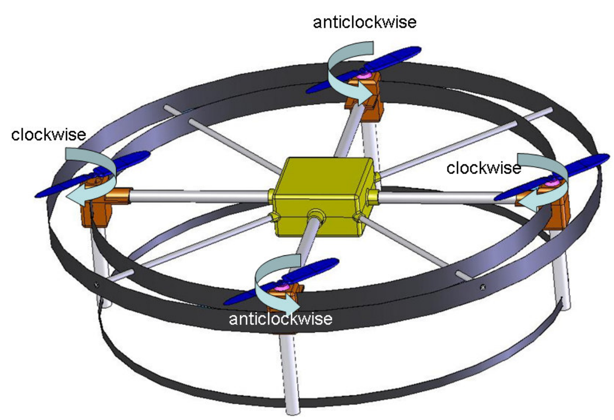

Figure 1: Second quad-rotor configuration

The second configuration is penalized by the structural weight, but it is definitely less prone to vibrations and bending, providing higher stiffness. In fact, the torsional stiffness of a closed section is substantially bigger than this of an opened frame section. To avoid small structure flexibility, the second configuration is chosen.

The structure was required to be simple, rugged and demountable. The goals for a MAVs has to make a system that can be used by a single operator and can stay in a backpack [7]. In order to minimize the weight, graphite bars are considered for the structure construction and a sandwich of fiber glass and Airex for the central body. The hub has to be designed to ensure the correct location and orientation of the struts on assembly and could be a simple under-over clamping system to provide a rugged demountable part.

For the prototype project the electric motors and the rotors was sourced from commercial RC equipment, for reasons of simplicity and practicality. The use or rigid rotors simplifies the aerodynamic modelling, even if it is possible that the external disturbances are increased.

In order to increase the safety vehicle, taking into account that the propellers are not protected, an external carbon fibre with a rectangular profile is adopted.

The characteristics of the reference aircraft are presented in Tab.1.

Table 1: Aircraft characteristics

Dimension	650x650 mm
Propeller size	254x120 mm
Structural weight	800 gr
Total weight	1300 gr
Payload weight	300/350 gr
Brushless engine	
Size	30x 37mm
Weight	55 gr
Speed controller	
Maximum	20 A
Weight	14 gr

Two propellers rotate anti-clockwise and the other two clockwise; in order to manoeuvre the aircraft is necessary to control the rotor speed. In particular, a control matrix must be designed to opportunely obtained the desired combination of attitude.
In hovering, all propellers must rotate with the same rotational speed. As a consequence, the thrust of all rotors must be equal and the torques have the same modulus but the opposite direction.

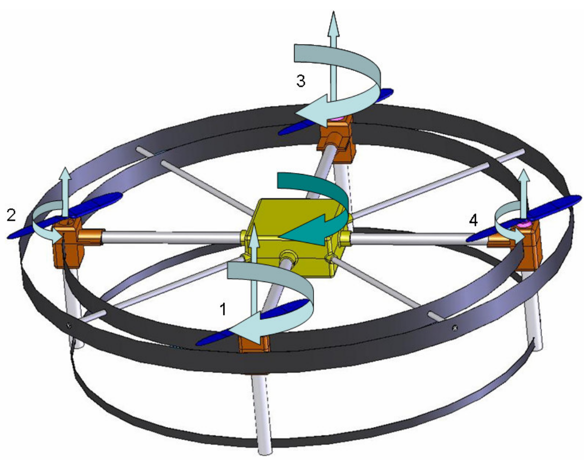

Figure 2: Hover control

For the forward flight, considering the first rotor has the displacement direction, the rotation is made around the pitch axis. The thrust on the rotor 3 is increased instead the thrust on the rotor 1 is decreased to maintain the equilibrium of the total torque. To move the platform in the right lateral side, the rotation is made around the roll axis and the thrust on rotor 2 is increased contemporarily the thrust on rotor 4 is decreased. The yaw is obtained increasing the thrust on the even rotors and decreasing the thrust on the odd ones, in order to maintain constant the altitude.

3.0 MATHEMATICAL MODEL

In order to analyze the dynamic behaviour of a multi rotor UAV and to evaluate the flight stability and quality, we consider a rigid blade model, neglecting the dynamic coupling between the rigid body and the structure flexibilities. This is due to the small vehicle dimensions and because we don't study the aeromechanics stability.
Taking into account the aerodynamics behaviour, each blade is dipped in an air field due to the combination of the rotational speed, the dragging speed and the inflow (due to the lift blade action).

Considering the model of a small four rotor, the inflow dynamics can be modelled as a uniform one, in this way:

$$\lambda = \frac{\sigma a}{16}\left(\sqrt{1+\frac{64}{3\sigma a}\vartheta_{0.75}}-1\right) \qquad (3.1)$$

where σ is the solidity ratio, a is the lift slope (usually 5.7) and $\vartheta_{0.75}$ is the blade pitch at 75% radius [8].
The twist is regarded linear, taking into account the simple mechanism of this quad-rotor:

$$\vartheta = \vartheta_0 + r\vartheta_{tw} \qquad (3.2)$$

where r is the radial location on the blade, measured from the centre of rotation to the blade tip, ϑ_0 is the command twist in which we consider the reliance on the angular velocity variation and ϑ_{tw} is the linear twist rate.
The mathematical model of the four rotor system includes the fuselage (the central body), the four principal rotors and the inflow of the principal rotors. The fuselage dynamics is modelled as a six d.o.f. rigid body, considering the Euler non linear equations. The blades and fuselage aerodynamics is considered linear.
The forces and moments of inertia for the blade infinitesimal elements are:

$$\begin{cases} d\vec{F}^i = -dm\cdot\vec{a}_P \\ d\vec{M}^i = \vec{r}_0\times d\vec{F}^i = -\vec{r}_0\times\vec{a}_P\cdot dm \end{cases} \qquad (3.3)$$

where $\vec{a}_P$ is the acceleration of the point P with an infinitesimal mass dm and $\vec{r}_0$ is the P-O vector in which O is the hinge point.
First of all, it is possible to model the blade as:

1. a thin layer with the mass equally distributed, taking into account the twist angle. In this case the twist angle is considered in the position vector of point P; so in the time derivative we have to consider also these variations, pointing out the coupling effects.
2. a thin bar with the mass equally distributed. In this case the coupling effects of feathering motion are neglected because the twist angle is considered constant in time.

In this case, we assume that the blade is modelled as a thin bar.

We consider the following reference frames [9]:

1. body reference frame (X_B,Y_B,Z_B): the origin is in the body centre of gravity; this is the reference frame related to the central body;
2. rotational reference frame (X_1,Y_1,Z_1): this reference frame rotates with the blade and X_1 lies in the same plane of the hub and the direction is related to the azimuth angle.
3. blade local reference frame (X_2,Y_2,Z_2): this reference frame rotates with the blade and X_2 is coincident with the longitudinal blade axis and Y_2 is perpendicular to X_2 in the rotation sense.

These reference frames are different if we consider the anticlockwise rotors or the other two. This is due because usually the rotation is positive when his direction is anticlockwise, so the reference frames are right-handed. Taking into account that every rotations must be right-handed (for an agreement).
We can observe the reference frames in the following figures.

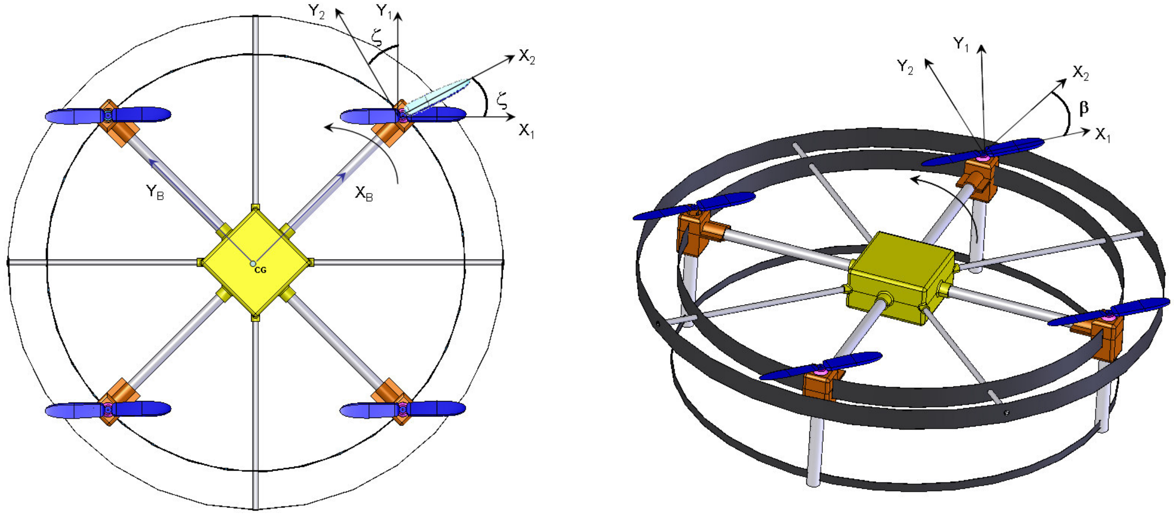

Figure 3: The reference frames on the anti-clockwise rotors

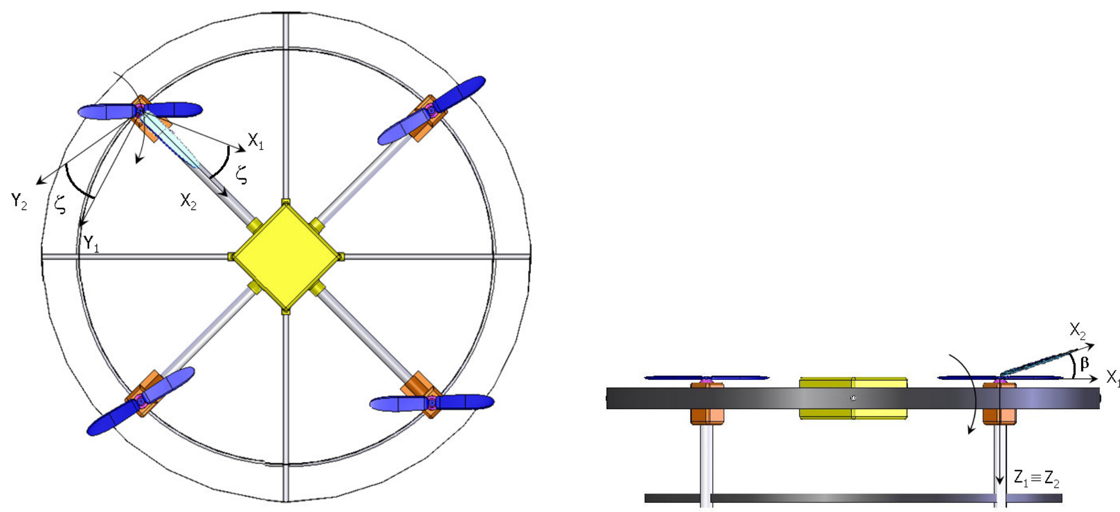

Figure 4: The reference frames on the clockwise rotors

Starting from the previous remarks, the rotor equations of motion differ in function of the spin direction. In fact, the transformation matrices between the rotational reference frame and the blade local one and between the rotational frame and the body one are different for the four rotors.

First, we consider the anticlockwise rotors and, in detail, the position vector of a generic point P, inside the blade, in the reference frame F_1. Assuming the blade as a thin bar, the position vector in the frame F_2 can be written as:

$$\vec{r}_P = \begin{bmatrix} r \\ 0 \\ 0 \end{bmatrix} \quad (3.4)$$

where r is the point coordinate along X_2. To obtain the vector in the reference frame F_1, two transformation matrices are applied.

A generic vector can be written as:

$$\vec{v}_1 = [A]_\beta [A]_\zeta \vec{v}_2 \qquad (3.5)$$

Taking into account the following transformation matrices

$$\begin{cases} [A]_\beta = \begin{bmatrix} \cos\beta & 0 & -\sin\beta \\ 0 & 1 & 0 \\ \sin\beta & 0 & \cos\beta \end{bmatrix} \\ [A]_\zeta = \begin{bmatrix} \cos\zeta & -\sin\zeta & 0 \\ \sin\zeta & \cos\zeta & 0 \\ 0 & 0 & 1 \end{bmatrix} \end{cases} \qquad (3.6)$$

the general vector is:

$$\vec{v}_1 = \begin{bmatrix} \cos\beta\cos\zeta & -\cos\beta\sin\zeta & -\sin\beta \\ \sin\zeta & \cos\zeta & 0 \\ \sin\beta\cos\zeta & -\sin\beta\sin\zeta & \cos\beta \end{bmatrix} \vec{v}_2 \qquad (3.7)$$

As indicated in the figures above, the zeta axes Z_1 and Z_2 are upwards.
The time derivative over the blade of the vector position is:

$$\frac{d}{dt}\vec{r}_P = \dot{\vec{r}}_P + \vec{\omega}_t \times \vec{r}_P \qquad (3.8)$$

The vector $\vec{\omega}_t$ represents the angular velocity of the reference frame. The first components are the angular velocity expressed in the reference frame F_1 and the third one is the hinge angular velocity expressed in the same frame.
We have the following matrix expression

$$\vec{V}'_P = \begin{bmatrix} -r\dot{\beta}\sin\beta\cos\zeta - r\dot{\zeta}\cos\beta\sin\zeta \\ r\dot{\zeta}\cos\zeta \\ r\dot{\beta}\cos\beta\cos\zeta - r\dot{\zeta}\sin\beta\sin\zeta \end{bmatrix} + \begin{bmatrix} p_1 \\ q_1 \\ \Omega \end{bmatrix} \times \begin{bmatrix} r\cos\beta\cos\zeta + e \\ r\sin\zeta \\ r\sin\beta\cos\zeta \end{bmatrix} \qquad (3.9)$$

Finally, the acceleration in the point P can be expressed as:

$$\vec{a}_P = \dot{\vec{V}}_P + \vec{\omega}_t \times \vec{V}_P \qquad (3.10)$$

Taking into account that for this vehicle the lag and the flap motions are constant, all the time derivatives of these two components are null. So the previous expressions can be simplified.
The angular velocity can be calculated starting from the body angular velocity.
A generic vector in the reference frame F_1, in function of the body axes, can be expressed as:

$$[\vec{v}]_I = [A]_\psi^{-1}[\vec{v}]_B \quad (3.11)$$

where the transformation matrix is obtained with two rotations (321). The first one is around the Z axis of an angle $(-\psi)$ and the second rotation is of an angle $(+180°)$ around the Y axis. Considering the rule of the rotation matrices, we obtained the following results:

$$\begin{cases} [A]_\psi = \begin{bmatrix} \cos\psi & \sin\psi & 0 \\ -\sin\psi & \cos\psi & 0 \\ 0 & 0 & 1 \end{bmatrix} \begin{bmatrix} -1 & 0 & 0 \\ 0 & 1 & 0 \\ 0 & 0 & -1 \end{bmatrix} = \begin{bmatrix} -\cos\psi & \sin\psi & 0 \\ \sin\psi & \cos\psi & 0 \\ 0 & 0 & -1 \end{bmatrix} \\ [A]_\psi^{-1} = \begin{bmatrix} -\cos\psi & \sin\psi & 0 \\ \sin\psi & \cos\psi & 0 \\ 0 & 0 & -1 \end{bmatrix} = \begin{bmatrix} -\cos\Omega t & \sin\Omega t & 0 \\ \sin\Omega t & \cos\Omega t & 0 \\ 0 & 0 & -1 \end{bmatrix} \end{cases} \quad (3.12)$$

In the specific case of the angular velocity, we have:

$$\begin{bmatrix} p_1 \\ q_1 \\ 0 \end{bmatrix} = \begin{bmatrix} -\cos\Omega t & \sin\Omega t & 0 \\ \sin\Omega t & \cos\Omega t & 0 \\ 0 & 0 & -1 \end{bmatrix} \begin{bmatrix} p \\ q \\ 0 \end{bmatrix} \Rightarrow \begin{cases} p_1 = -p\cos\Omega t + q\sin\Omega t \\ q_1 = p\sin\Omega t + q\cos\Omega t \end{cases} \quad (3.13)$$

The time derivatives are:

$$\begin{cases} \dot{p}_1 = -\dot{p}\cos\Omega t + p\Omega\sin\Omega t + \dot{q}\sin\Omega t + q\Omega\cos\Omega t \\ \dot{q}_1 = \dot{p}\sin\Omega t + p\Omega\cos\Omega t + \dot{q}\cos\Omega t - q\Omega\sin\Omega t \end{cases} \quad (3.14)$$

We are considering the trim conditions where the linear and angular velocities are zero (steady state condition).

In order to obtain the aerodynamic and inertial actions, we have to transform the velocities and the accelerations in the blade local reference frame.
As said before, a generic vector can be transformed in the following way

$$\vec{v}_1 = [A]_\beta [A]_\zeta \vec{v}_2 \quad (3.15)$$

So the velocities and the accelerations becomes

$$\begin{cases} \vec{V}_{P2} = \{[A]_\beta [A]_\zeta\}^T \cdot \vec{V}_{P1} \\ \vec{a}_{P2} = \{[A]_\beta [A]_\zeta\}^T \cdot \vec{a}_{P1} \end{cases} \quad (3.16)$$

The inertial moment along the axis X_2 is zero due to the system model (modelled as a thin bar).
Integrating along the blade starting from the hinge point, we obtain the force and moment resultants.
The integration must be do along the non-dimensional radial coordinate x. For this reason, the infinitesimal mass dm must be rewritten as the mass per unit length η; so we obtain the following relationship:

$$\begin{cases} dm = \eta R dx \\ r \cdot dm = \eta R^2 x dx \end{cases} \quad (3.17)$$

The final expressions are:

$$\vec{F}^i = \begin{bmatrix} -\eta R \int_0^1 a_{PX2} \cdot dx \\ -\eta R \int_0^1 a_{PY2} \cdot dx \\ -\eta R \int_0^1 a_{PZ2} \cdot dx \end{bmatrix} = \begin{bmatrix} F^i_{X_2} \\ F^i_{Y_2} \\ F^i_{Z_2} \end{bmatrix} \quad (3.18)$$

$$\vec{M}^i = \begin{bmatrix} 0 \\ \eta R^2 \int_0^1 a_{PZ2} \cdot xdx \\ -\eta R^2 \int_0^1 a_{PY2} \cdot xdx \end{bmatrix} = \begin{bmatrix} M^i_{X_2} \\ M^i_{Y_2} \\ M^i_{Z_2} \end{bmatrix} \quad (3.19)$$

In order to obtain the force and moment resultants, we have to calculate the airspeed with respect to one blade point, in the reference frame F_2. The flux speed with respect to the blade is a vector sum of three terms:

1. the speed due to the azimuth, lag and flap motions.
2. the vehicle dragging speed, that is expressed in body axes, so this speed must to be transformed in the reference frame F_1, considering the transformation matrix $[A]_\psi^{-1}$.
3. the rotor inflow is expressed in the non-rotating axes (coincident with the body axes); we consider again the matrix $[A]_\psi^{-1}$. This last term is calculated in the following way:

$$W_i = \Omega R_D \lambda_i \quad (3.20)$$

where R_D is the actuator disc radius and λ_i is the inflow coefficient. As said before the inflow is consider uniform.

The flux speed with respect to the blade, considering all the components, is the difference between all the terms.

These components must be transformed in the reference frame F_2, in order to obtain the radial, parallel and perpendicular components of the relative speed along the infinitesimal blade in the neighborhood of the point P.

We have to calculate the infinitesimal lift and drag, using the momentum-blade element theory. We consider the following force and speed distribution.

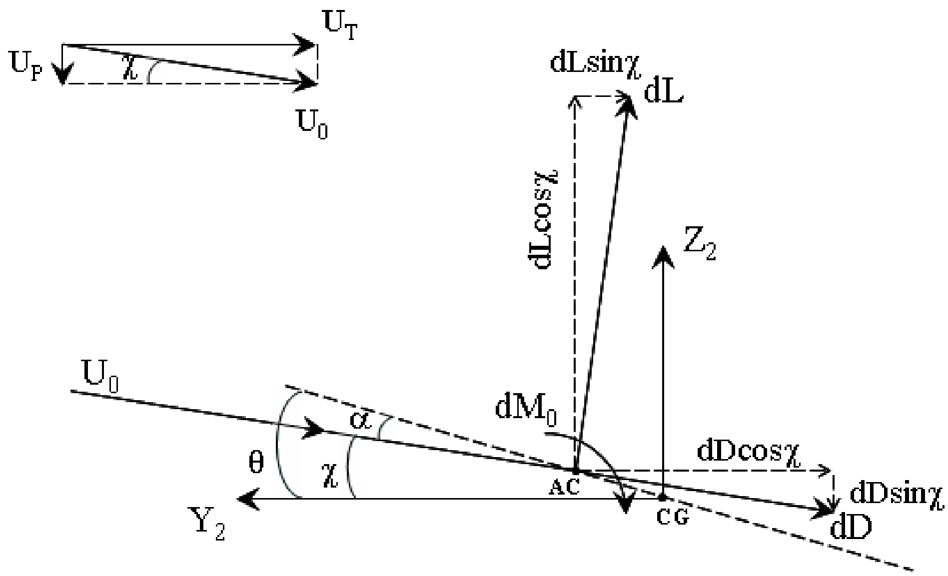

Figure 5: Momentum blade element theory for anti-clockwise rotors

The infinitesimal lift and drag and the focal moment M_0 act on the aerodynamic centre. In the equilibrium the moment is considered zero, instead the lift and drag forces are:

$$\begin{cases} dL = \dfrac{1}{2}\rho U_0^2 C_L dS = \dfrac{1}{2}\rho\left(U_T^2 + U_P^2\right)C_L dS \\ dD = \dfrac{1}{2}\rho U_0^2 C_D dS = \dfrac{1}{2}\rho\left(U_T^2 + U_P^2\right)C_D dS \end{cases} \quad (3.21)$$

The infinitesimal surface can be expressed as a function of the blade chord and of the non-dimensional radial coordinate x, in fact we have: $dS = cR \cdot dx$.
The lift and drag components must to be calculated in the reference frame F_2, so we have to consider the value with respect to the Y_2 and Z_2 axes.
dependence from the azimuth angle and the blade rotation.
The aerodynamic and inertial forces must be transformed in the reference frame F_1.

$$\begin{bmatrix} F^A_{X1} \\ F^A_{Y1} \\ F^A_{Z1} \end{bmatrix} = \begin{bmatrix} \cos\beta\cos\zeta & -\cos\beta\sin\zeta & -\sin\beta \\ \sin\zeta & \cos\zeta & 0 \\ \sin\beta\cos\zeta & -\sin\beta\sin\zeta & \cos\beta \end{bmatrix} \begin{bmatrix} 0 \\ F^A_{Y2} \\ F^A_{Z2} \end{bmatrix} \quad (3.22)$$

$$\begin{bmatrix} F^i_{X1} \\ F^i_{Y1} \\ F^i_{Z1} \end{bmatrix} = \begin{bmatrix} \cos\beta\cos\zeta & -\cos\beta\sin\zeta & -\sin\beta \\ \sin\zeta & \cos\zeta & 0 \\ \sin\beta\cos\zeta & -\sin\beta\sin\zeta & \cos\beta \end{bmatrix} \begin{bmatrix} F^i_{X_2} \\ F^i_{Y_2} \\ F^i_{Z_2} \end{bmatrix} \quad (3.23)$$

As you can see, these forces are dependent by the azimuth angle.
In the same way, we can calculate the aerodynamic and inertial moments for the reference frame F_1.
These forces and moments must be transformed in body axes.
In order to obtain the forces and moments given to the hub by all the blades, we have to calculate the average actions and we have to multiply considering the blade number. The aerodynamic and inertial

resultants are obtained in this way:

$$\begin{cases} X_R^i = \frac{1}{\pi}\int_0^{2\pi} F_{XB}^i(\psi)d\psi \\ Y_R^i = \frac{1}{\pi}\int_0^{2\pi} F_{YB}^i(\psi)d\psi \\ Z_R^i = \frac{1}{\pi}\int_0^{2\pi} F_{ZB}^i(\psi)d\psi \end{cases} \qquad \begin{cases} L_R^i = \frac{1}{\pi}\int_0^{2\pi} M_{XB}^i(\psi)d\psi \\ M_R^i = \frac{1}{\pi}\int_0^{2\pi} M_{YB}^i(\psi)d\psi \\ N_R^i = \frac{1}{\pi}\int_0^{2\pi} M_{ZB}^i(\psi)d\psi \end{cases} \quad (3.24)$$

$$\begin{cases} X_R^A = \frac{1}{\pi}\int_0^{2\pi} F_{XB}^A(\psi)d\psi \\ Y_R^A = \frac{1}{\pi}\int_0^{2\pi} F_{YB}^A(\psi)d\psi \\ Z_R^A = \frac{1}{\pi}\int_0^{2\pi} F_{ZB}^A(\psi)d\psi \end{cases} \qquad \begin{cases} L_R^A = \frac{1}{\pi}\int_0^{2\pi} M_{XB}^A(\psi)d\psi \\ M_R^A = \frac{1}{\pi}\int_0^{2\pi} M_{YB}^A(\psi)d\psi \\ N_R^A = \frac{1}{\pi}\int_0^{2\pi} M_{ZB}^A(\psi)d\psi \end{cases} \quad (3.25)$$

As said before, these remark can be evaluate only for the counter-clockwise rotors. In general, the assumptions adopted for the other two rotors hold yet true, but the transformation matrices vary in the following way.
For example, a generic vector can be written as:

$$\vec{v}_1 = [A]_\beta [A]_\zeta \vec{v}_2 \quad (3.26)$$

For a clockwise rotation, to obtain a vector from the reference frame F_1 to the frame F_2 we have to consider two rotations (rotation order: 232):

1. first rotation around the Y axis of an angle β;
2. second rotation around Z axis of an angle ζ.

So, the transformation matrices are:

$$\begin{cases} [A_2]_\beta = \begin{bmatrix} \cos\beta & 0 & \sin\beta \\ 0 & 1 & 0 \\ -\sin\beta & 0 & \cos\beta \end{bmatrix} \\ [A_2]_\zeta = \begin{bmatrix} \cos\zeta & -\sin\zeta & 0 \\ \sin\zeta & \cos\zeta & 0 \\ 0 & 0 & 1 \end{bmatrix} \end{cases} \quad (3.27)$$

For a clockwise rotor only one rotation is necessary in order to align the rotational reference frame F_1 and the body axes, taking into account a rotation order 321. indeed, it is sufficient a single rotation around the Z axis of an angle ψ.
As for the anti-clockwise rotor, in order to obtain the force and moment resultants, we have to calculate the flux speed with respect to the blade as a sum of three terms:

1. the speed due to the azimuth, lag and flap motions.

2. the vehicle dragging speed, that is expressed in body axes.

3. the rotor inflow is expressed in the non-rotating axes (coincident with the body axes); we consider again the matrix $[A_2]_\psi^{-1}$. This last term is calculated as said before (Eqs. 3.1 and 3.20).

We have to calculate the infinitesimal lift and drag, using the momentum-blade element theory. Due to the different reference frames, we consider the following force and speed distribution.

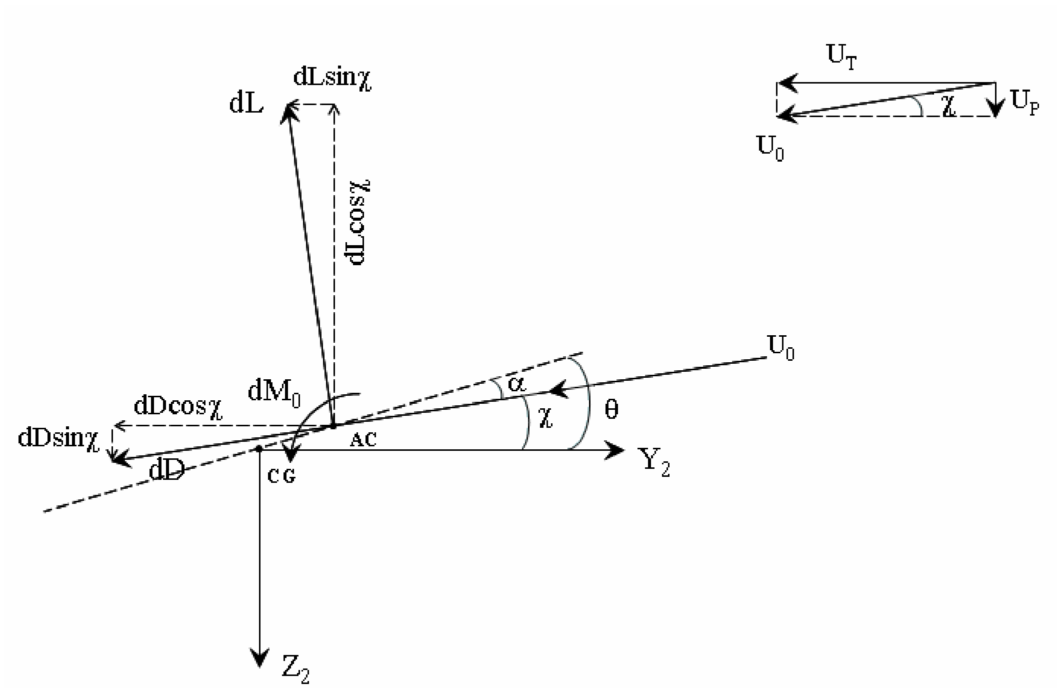

Figure 6: Momentum blade element theory for the clockwise rotors

The infinitesimal lift and drag and the focal moment M_0 act on the aerodynamic centre.

The lift and drag components must to be calculated in the reference frame F_2, so we have to consider the value with respect to the Y_2 and Z_2 axes.

Considering the force distribution in Fig. 1, the infinitesimal aerodynamic force is:

$$d\vec{F}^A = \begin{bmatrix} 0 \\ d\vec{F}^A_{Y2} \\ d\vec{F}^A_{Z2} \end{bmatrix} = \begin{bmatrix} 0 \\ -dL\sin\chi - dD\cos\chi \\ -dL\cos\chi + dD\sin\chi \end{bmatrix} \quad (3.28)$$

In order to evaluate the complete mathematical model for a quad-rotor, we have to consider the fuselage equations of motion [10]. The rigid body equation are:

$$\begin{cases} \vec{R}^a + \vec{R}^i = \vec{R}^a - \dfrac{d}{dt}\vec{Q} = 0 \\ \vec{M}^a + \vec{M}^i = \vec{M}^a - \dfrac{d}{dt}\vec{K}_g = 0 \end{cases} \quad (3.29)$$

where $\vec{Q} = m\vec{V}_g$ is the momentum of momentum vector, $\vec{V}_g = U \cdot \hat{i}_B + V \cdot \hat{j}_B + W \cdot \hat{k}_B$ is the centre of

gravity speed and $\vec{K}_g = [I]_g \cdot \vec{\omega}_e$ is the angular momentum.
In particular,

$$\vec{K}_g = \begin{bmatrix} I_{XX} & 0 & -I_{XZ} \\ 0 & I_{YY} & 0 \\ -I_{ZX} & 0 & I_{ZZ} \end{bmatrix} \cdot \vec{\omega}_e = \begin{bmatrix} I_{XX}p - I_{XZ}r \\ I_{YY}q \\ I_{ZZ}r - I_{ZX}p \end{bmatrix} \quad (3.30)$$

with $\vec{\omega}_e$ is the vehicle angular velocity in the body reference frame.
The time derivative of the two momentum are:

$$\begin{cases} \frac{d}{dt}\vec{Q} = \dot{\vec{Q}} + \vec{\omega}_t \times \vec{Q} \\ \frac{d}{dt}\vec{K}_g = \dot{\vec{K}}_g + \vec{\omega}_t \times \vec{K}_g \end{cases} \quad (3.31)$$

The angular velocity $\vec{\omega}_t$ is the velocity of the body frame with respect to an inertial one; this velocity is coincident with the vehicle angular velocity, so $\vec{\omega}_e \equiv \vec{\omega}_t = p \cdot \hat{i}_B + q \cdot \hat{j}_B + r \cdot \hat{k}_B$.
The inertial resultant can be evaluate calculating the time derivative of the $\vec{Q}$ and $\vec{K}_g$ vectors and the cross product indicated in the above equation.
So we obtain:

$$\begin{cases} \dot{\vec{Q}} = \begin{pmatrix} m\dot{U} \\ m\dot{V} \\ m\dot{W} \end{pmatrix} \\ \vec{\omega}_t \times \vec{Q} = \begin{vmatrix} \hat{i}_B & \hat{j}_B & \hat{k}_B \\ p & q & r \\ mU & mV & mW \end{vmatrix} = \begin{pmatrix} m(qW - rV) \\ m(rU - pW) \\ m(pV - qU) \end{pmatrix} \\ \frac{d}{dt}\vec{Q} = \begin{pmatrix} m(\dot{U} + qW - rV) \\ m(\dot{V} + rU - pW) \\ m(\dot{W} + pV - qU) \end{pmatrix} \end{cases} \quad (3.32)$$

The time derivative of inertial vector $\vec{K}_g$ and the cross product are calculated as:

$$\frac{d}{dt}\vec{K}_g = \begin{pmatrix} I_{XX}\dot{p} - I_{XZ}\dot{r} + rq(I_{ZZ} - I_{YY}) - pqI_{ZX} \\ I_{YY}\dot{q} + I_{ZX}(p^2 - r^2) + pr(I_{XX} - I_{ZZ}) \\ I_{ZZ}\dot{r} - I_{ZX}\dot{p} + pq(I_{YY} - I_{XX}) + I_{XZ}qr \end{pmatrix} \quad (3.33)$$

The vector $\vec{R}^a$ is relative to the active forces acting on the fuselage

$$\vec{R}^{a} = \vec{R} + \vec{R}_{A} + \vec{R}_{g} \qquad (3.34)$$

where $\vec{R} = X \cdot \hat{i}_B + Y \cdot \hat{j}_B + Z \cdot \hat{k}_B$ is the aerodynamic and inertial resultant of the rotor forces exchanged with the fuselage, $\vec{R}_A = X_A \cdot \hat{i}_B + Y_A \cdot \hat{j}_B + Z_A \cdot \hat{k}_B$ is the aerodynamic fuselage resultant and $\vec{R}_g = mg_X \cdot \hat{i}_B + mg_Y \cdot \hat{j}_B + mg_Z \cdot \hat{k}_B$ is the weight fuselage resultant.
In analogy, the active moments on the fuselage are

$$\vec{M}^{a} = \vec{M}_{t} + \vec{M}_{A} \qquad (3.35)$$

where $\vec{M}_t = L_t \cdot \hat{i}_B + M_t \cdot \hat{j}_B + N_t \cdot \hat{k}_B$ is the transport moment resultant, $\vec{M}_A = L_A \cdot \hat{i}_B + M_A \cdot \hat{j}_B + N_A \cdot \hat{k}_B$ is the aerodynamic fuselage resultant.
The gravity vector, known in the vertical axes, must be transformed in the body frame taking into account the transformation matrix

$$[T]_{BV} = \begin{bmatrix} \cos\Psi\cos\Theta & \sin\Psi\cos\Theta & -\sin\Theta \\ -\sin\Psi\cos\Phi + \cos\Psi\sin\Theta\sin\Phi & \cos\Psi\cos\Phi + \sin\Psi\sin\Theta\sin\Phi & \cos\Theta\sin\Phi \\ \sin\Psi\sin\Phi + \cos\Psi\sin\Theta\cos\Phi & -\cos\Psi\sin\Phi + \sin\Psi\sin\Theta\cos\Phi & \cos\Theta\cos\Phi \end{bmatrix} \qquad (3.36)$$

In conclusion we can write the force and moment equations.

$$\begin{cases} X + X_A = m(\dot{U} + qW - rV) + mg\sin\Theta \\ Y + Y_A = m(\dot{V} + rU - pW) - mg\cos\Theta\sin\Phi \\ Z + Z_A = m(\dot{W} + pV - qU) - mg\cos\Theta\cos\Phi \end{cases} \qquad (3.37)$$

$$\begin{cases} L_t + L_A = I_{XX}\dot{p} - I_{XZ}\dot{r} + rq(I_{ZZ} - I_{YY}) - pqI_{ZX} \\ M_t + M_A = I_{YY}\dot{q} + I_{ZX}(p^2 - r^2) + pr(I_{XX} - I_{ZZ}) \\ N_t + N_A = I_{ZZ}\dot{r} - I_{ZX}\dot{p} + pq(I_{YY} - I_{XX}) + I_{XZ}qr \end{cases} \qquad (3.38)$$

In order to complete the equation system, we have to evacuate the correlation between the Euler angles and the vehicle angular velocity. We have to consider the kinematic equations:

$$\begin{cases} p = \dot{\Phi} - \dot{\Psi}\sin\Theta \\ q = \dot{\Theta}\cos\Phi + \dot{\Psi}\cos\Theta\sin\Phi \\ r = -\dot{\Theta}\sin\Phi + \dot{\Psi}\cos\Theta\cos\Phi \end{cases} \qquad (3.39)$$

4.0 ANALYSIS OF THE HOVER CONDITION

We would like to analyze the hover condition; so we have to simplify the equations. In hover, the vehicle speeds are zero and, as a consequence, all the fuselage aerodynamic effects are zero. So we have:

$$\begin{pmatrix} U \\ V \\ W \end{pmatrix} = 0 \quad \Rightarrow \quad \begin{pmatrix} X_A \\ Y_A \\ Z_A \end{pmatrix} = 0 \quad \begin{pmatrix} L_A \\ M_A \\ N_A \end{pmatrix} = 0 \qquad (4.1)$$

In this case the turn rate is zero so the heading is constant: $\dot{\Psi} = 0$.
As a consequence, the angular velocities are null, but, in the general situation, the attitude angle and the roll one are different from zero.
The force and moment equations are function of the angular rotation Ω. In general conditions the four angular rotation are different, but in hovering these become $\Omega_1 = \Omega_3 = -\Omega_2 = -\Omega_4$, so we have to consider this simplification in the equations of motion.

This model is implemented in Matlab –Simulink® program, in order to evaluate the dynamic stability of the system.

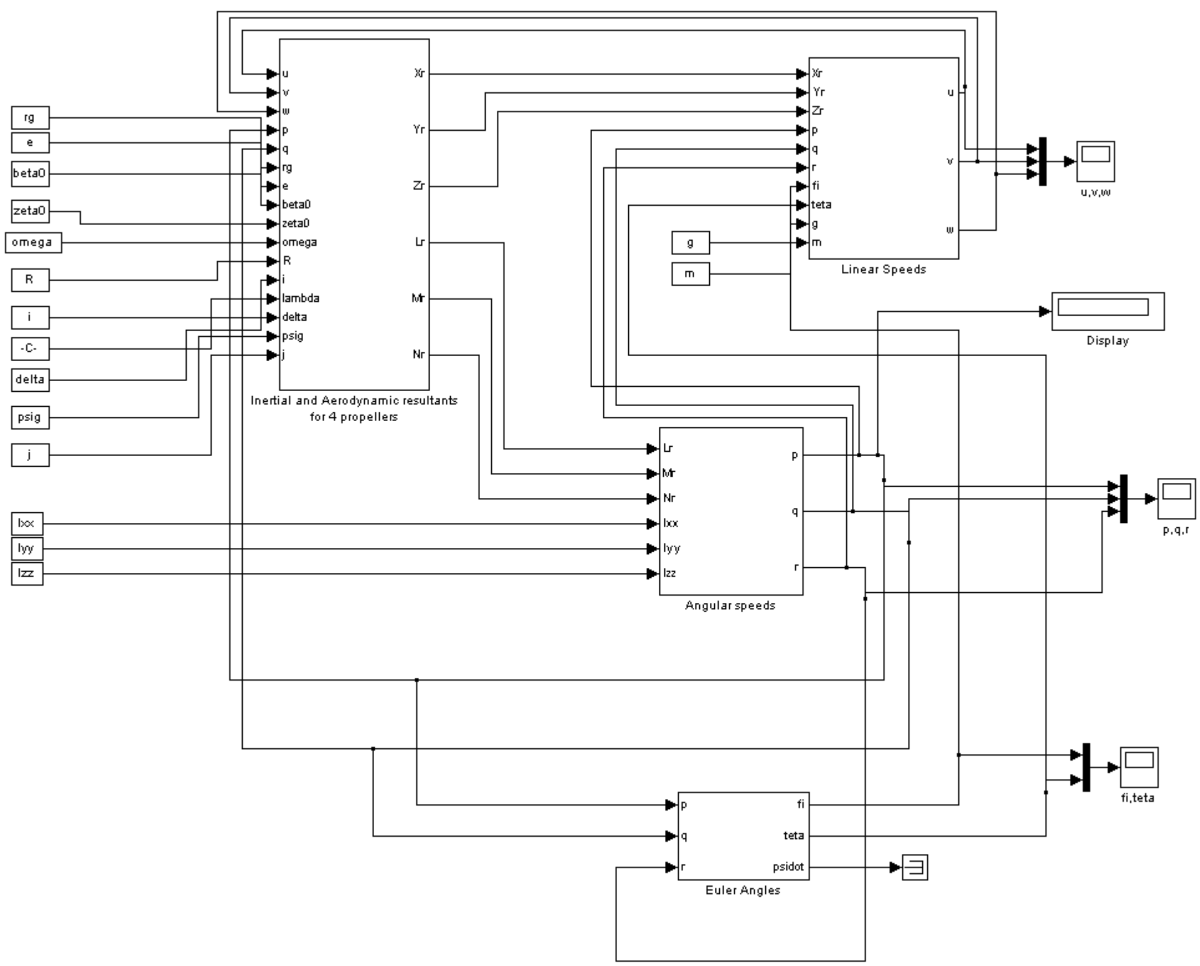

Figure 7: Model impletation in Simulink

We impose an initial rotor angular rotation, in order to verify the platform stability.
Without a controller, the system diverge after wide parameters oscillations. So the system must be controlled.

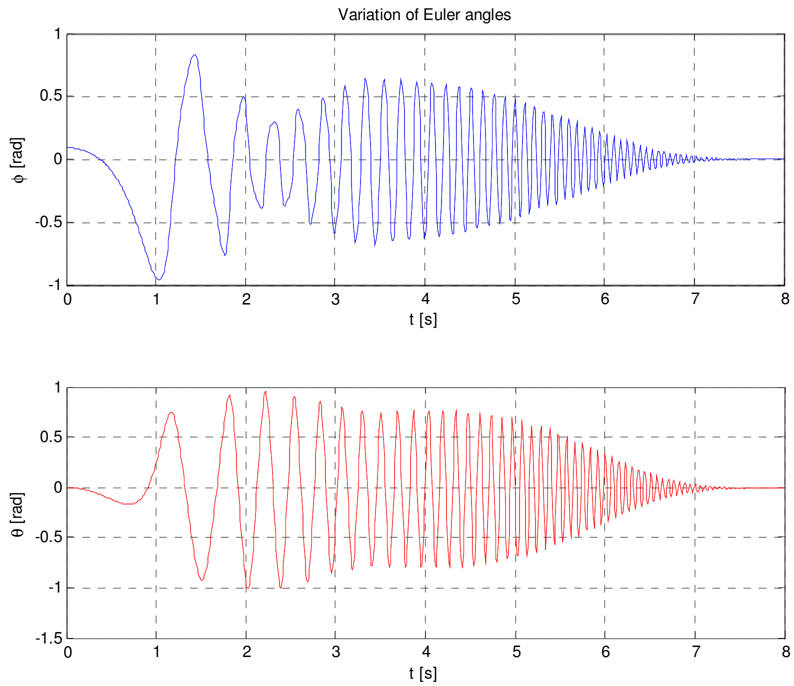

Figure 8: Variation of the Euler angles

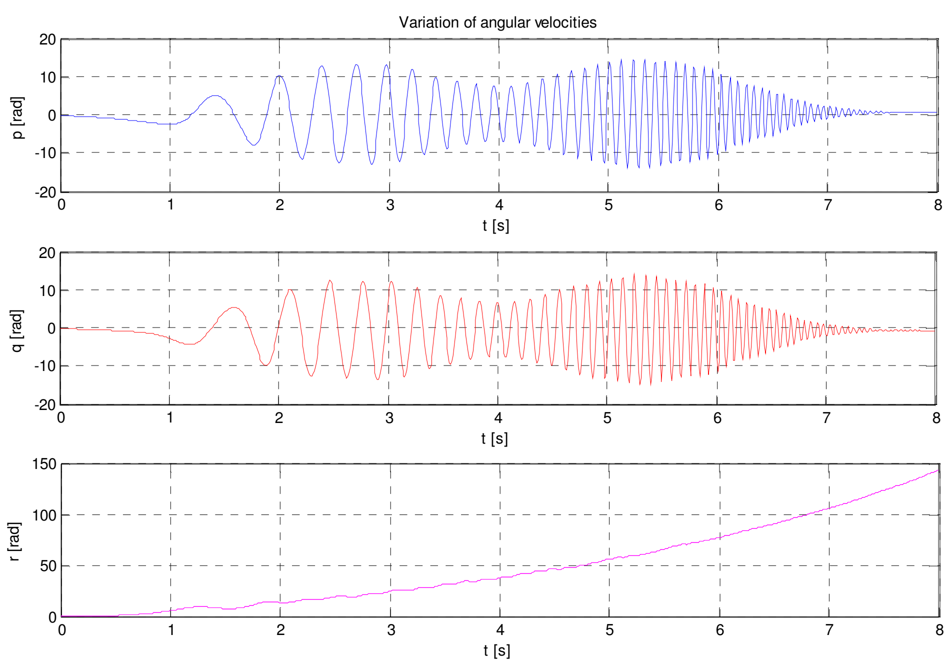

Figure 9: Variation of the angular speed

The input control of our system is the rotor angular rotation, so, in order to stabilize the platform, it can be necessary to control the variation of the rotor angular speed.

Considering the control laws of the quad-rotor, the variation of the angular speeds is controlled by the change of the angular velocities p,q,r.
We have imposed as initial condition that the differential variation sum of the fourth blade rotations is zero.

The platform must be stable after a given disturbance, moving back to the attitude initial conditions.
With a trial and error method we have to define the gains, correlated to the angular velocities. We impose a perturbation of five degrees on the roll angle.
To damp the oscillation and to reduce the steady state error, a PD controller is necessary.
The following results have been obtained.

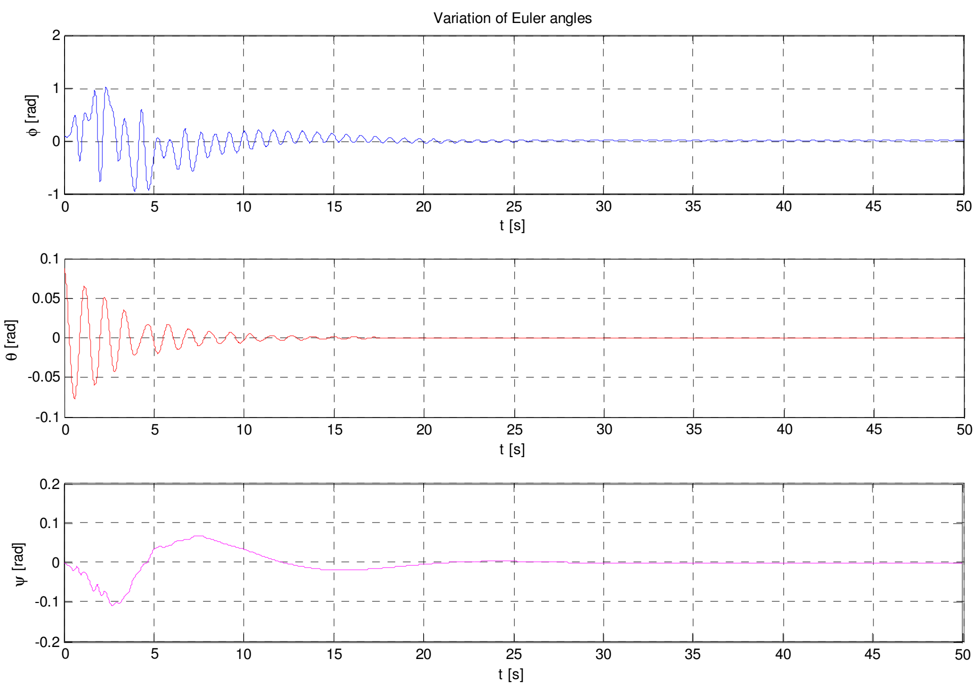

Figure 10: Variation of Euler angles with a PD controller

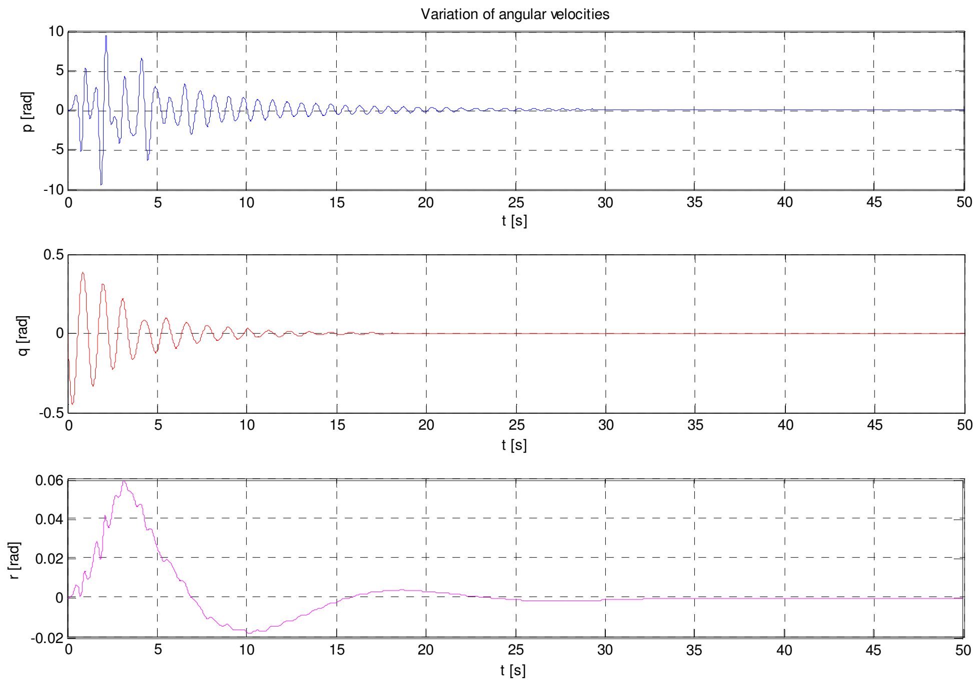

Figure 11: Variation of the angular velocities with a PD controller

After the gain tuning, starting from an absolute rotor angular rotation in hovering of 10 rad/s, the four resulting angular speeds are:

$$\begin{cases} \Omega_1 = 10.12 \ \ \mathrm{rad/s} \\ \Omega_2 = -10.00 \ \ \mathrm{rad/s} \\ \Omega_3 = 9.916 \ \ \mathrm{rad/s} \\ \Omega_4 = -10.03 \ \ \mathrm{rad/s} \end{cases}$$

The implementation of the model with an integrative gain increases the system oscillation, without improving the rise time of the system and the steady state error.
The requirements for this kind of platform are: the rise time has to be less than 5 seconds, the overshoot under the 5% and the steady state error under the 2%. In order to obtained these results an optimal regulation has to be implemented.

5.0 CONCLUSIONS

In this paper a quad-rotor prototype has been designed using commercial and COTS components. The electric and structural parts are defined optimizing the platform stiffness and providing rugged system, not neglecting the total aircraft weight.

The exploration of the mathematical model of the vehicle is also outlined, taking into account the dynamic model of the fuselage and of the four rotors. Some results are obtained analyzing the hover conditions. We can demonstrate that a proportional controller on Euler angles does not guarantee stable conditions.

The response is dynamically stable and, after a perturbation, the aircraft is moving back to the trim conditions. As a future research the response can be optimized and the closed-loop system can be asymptotically stable, this is possible with a complete gain matrix K and an LQR controller. In fact the LQR controllers are also inherently robust with respect to process uncertainty.

The next step includes the construction of a prototype rotorcraft, in order to validate the stability characteristics in remote control. With the controller board we can demonstrate if the gain matrix K obtained is compatible or if another gain tuning is required.
At the same time, the model of the remote controller has to be implemented in the complete block diagram, so as to reproduce as faithfully as possible the real system. In this way, the model input is the real one.

1. References

[1] Conroy, J.K., Samuel, P.D., Pines, D.J., "Development of a MAV Control and Navigation System", AIAA Infotech@Aerospace Conference, Arlington (Virginia), 26 - 29 Sep 2005.

[2] McKerrow, P., "Modelling the Draganflyer four-rotor helicopter", 2004 IEEE International Conference on Robotics and Automation, New Orleans (LA, USA), 26 April-1May 2004.

[3] Arning, R.K., Sassen, S., "Flight Control of Micro Aerial Vechicles", AIAA Guidance Navigation and Control Conference and Exhibit, Providence (Rhode Island), 16-19 Aug. 2004.

[4] Pounds, P., Mahony, R., Gresham, J., Corke, P., Roberts, J., "Towards Dynamically-Favourable Quad-Rotor Aerial Robots", Australasian Conference on Robotics and Automation, Canberra (Australia), 6-8 Dec. 2004.

[5] Castillo, P., Dzul, A., Lozano, R., "Real-Time Stabilization and Tracking of a Four-Rotor Mini Rotorcraft", IEEE Transactions on Control Systems Technology, volume 12, pages 510–6, July 2004.

[6] Earl, M. G., D'Andrea, R., "Real-Time Attitude Estimation Techniques Applied to a Four Rotor Helicopter", 43rd IEEE Conference on Decision and Control, Bahamas, 14-17 Dec. 2004.

[7] Office of the Secretary of Defense, "Unmanned Aircraft Systems Roadmap: 2005-2030", 2005

[8] Johnson, W., "Helicopter Theory", Dover Publications inc, 1980

[9] Talbot, P.D., Tinling, B.E., Decker, W.A., Chen, R.T.N., "A mathematical model of a single main rotor helicopter for piloted simulation", National Aeronautics and Space Administration, NASA Technical Memorandum 84281, September 1982

[10] Mouhingou, A., Azouz, N., "Modelling of a flexible quadrirotor helicopter", AMSE 2006 International Design Engineering Technical Conference & Computers and Information in Engineering Conference, September 10-13 2006, Philadelphia, Pennsylvania, USA